

Thermodynamics modeling for moving contact line in gas/liquid/solid system: Capillary rise problem revisited

H. Fan, Y. X. Gao, and X. Y. Huang

School of Mechanical and Production Engineering, Nanyang Technological University, Singapore 639798, Republic of Singapore

(Received 19 May 2000; accepted 17 February 2001)

The nonequilibrium thermodynamics framework is tailored in the present paper to formulate the gas/liquid/solid system. In this system, there are two important issues, namely, the contact line motion and contact angle change, and shear stress singularity, during the dynamic evolution. Traditionally, the fluid mechanics approach has been applied to model these two issues. In the present paper, we applied a thermodynamics formulation to re-examine the first issue, i.e., the dynamic motion of the contact line and angle, and which provides a new angle to understand the fundamentals of this classical problem. In order to verify the reliability of the present thermodynamics formulation, the capillary rise problem is revisited by using the formulation. A numerical result obtained based on the thermodynamics formulation is then compared with an experimental test data. Excellent agreement between our analytical and experimental results gives us confidence for the future works on this approach. © 2001 American Institute of Physics.
[DOI: 10.1063/1.1369140]

I. INTRODUCTION

The gas/liquid/solid system is encountered in many well-known configurations, for example, a liquid droplet spreading on a smooth solid surface, liquid column rises in a capillary tube, and liquid trapped in a solid corner, to name a few. All these configurations have a common nature, that is, the surface tension dominates the evolution process as the size of the liquid domain is small. Needless to say, the theoretical value of understanding the system is of importance. On top of that, there are numerous applications in modern industries directly depending on the research outcomes of this problem. Therefore, it is not surprised that the problem has attracted tremendous interest from the theoretical researchers as well as practical engineers. A thorough and detailed review on this topic could be difficult since it has been an active research area in the past three decades. What we tried in this Introduction is to briefly review the most recent and important contributions to this topic, which gives us the confidence that the following thermodynamics model is fresh and a new approach of analyzing the problem.

Let us first unify our terminology in the following discussion for the gas/liquid/solid system illustrated by Fig. 1(a). For example, a liquid droplet spreading on a solid surface [Fig. 1(c)] is one of the gas/liquid/solid systems. The contact line is the conjunction line of gas/liquid/solid commonly shared, which is sometimes called the triple point line (TPL). The contact angle is the angle between the solid/liquid interface and liquid/gas interface. At the equilibrium state (or static state), the gas/liquid interface is described by the Laplace equation and the static contact angle is obtained via the Young's equation. What we are interested as well as all the researchers in the past two decades are the dynamic evolution of the contact line and the contact angle.

The majority of the contributions up to date was made by fluid mechanics researchers. We found that Shikhmurzaev's paper¹ on this topic not only proposed a fresh model for deriving the contact line motion and contact angle change, but also made a thorough review (over 80 references were listed in his paper) on the related models. Interested readers are suggested to read Sec. IX of his paper for the detailed and in depth review. Hereby, we only briefly go through the main points included in all the fluid mechanics based models, as Shikhmurzaev reviewed. From there we introduce a totally different approach to exam the gas/liquid/sold system via the nonequilibrium thermodynamics formation.

The main effort made from the fluid mechanics point of view is to understand two unfamiliar phenomena to the classical fluid mechanics. The first is that the relationship between the moving velocity of the contact line and the changing of contact angle is not described by the conventional fluid mechanics governing equations. A model was needed, or alternatively, an empirical relation between the velocity of the contact line and the instant contact angle was posted to proceed the fluid mechanics calculation for the whole field. One of these empirical relations is

$$V = k(\theta - \theta_e)^m, \quad (1.1)$$

where θ_e is the equilibrium contact angle; k and m are empirically determined constants for the configurations under consideration (see, e.g., Refs. 2–3). However, it was noticed that k and m , determined from one geometric configuration, might not be suitable for the other configurations. Therefore, it may be argued that the expression of Eq. (1.1) and its equivalents are not constitutive relations, rather an experimental relation.

The second important issue discussed by the fluid mechanics models was the singular shear stress near the corner

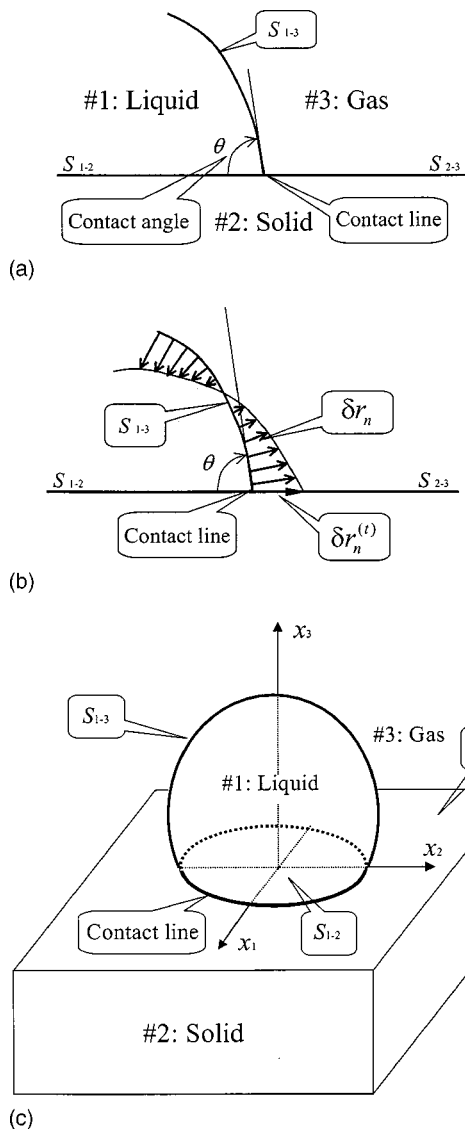


FIG. 1. (a) Contact line and interfaces in a gas/liquid/solid system. (b) The interface S_{1-3} or the contact line undergoes a virtual motion δr_n or $\delta r_n^{(t)}$. (c) A liquid droplet spreading on a solid.

of the contact line. This singularity is not acceptable from the physics point of view. Various models and assumptions were proposed to eliminate this singularity. The basic approach of making the models for eliminating the singularity is to construct boundary layers so that the asymptotic field near the contact line is regular (see, e.g., Refs. 1, 2, 4, 5). A matching technique is needed for the inner and outer region solutions.

In the following sections, we introduce a nonequilibrium thermodynamics framework with which the evolution process is proceeded in the direction of lowering the total free energy of the whole system. Speaking of the system, we extend the system to include the fluid, all interfaces, and the triple point line (TPL). The free energy should include the conventional energies in the fluid mechanics, and also all the surface energies on the all the interfaces (gas/liquid, liquid/solid, and gas/solid). It will be seen that the thermodynamics formulation provides a set of constitutive equations for the gas/liquid interface and contact line. It has a sound thermo-

dynamics foundation and can replace all the empirical laws, such as Eq. (1.1). As to the second issue of the modeling via the fluid mechanics approach, namely the singularity issue, we have to adopt the existing results obtained in the past two decades. The inclusion of the interfaces and TPL in the thermodynamics formulation does not resolve the shear stress singularity inside the liquid phase where the fluid mechanics prevails. Apparently, the interface and TPL evolution and fluid field variables are coupled in the same problem under this unified energy formulation. Uncoupling the fluid field solution and interface evolution process requires certain simplifications with reasonable and practical arguments.

It is noticed that quite a few engineering applications concern the contact line motion and contact angle change only. The details of the fluid in the immediate vicinity of the contact line is not of interest to the engineers. For example, when people study the molten solder spreading on the microscopic scale in the modern electronic packaging process, only the contact line and contact angle evolution was concerned.⁶ On the other hand, from the analytical point of view, the fluid field variables can be simplified when the energies associated with these terms are orders of magnitude smaller than those contributed from interface energies. Under this circumstance, we can simplify the field solutions inside of the liquid so that only the interface and triple point line (TPL) are included in our free energy. The effect of the liquid is then taken into account via the Laplace pressure across the liquid/gas interface, as shown in our calculations in the following sections for the capillary rise problem. We employed this scheme, with a simplified fluid field solution, to analyze the solder droplet spreading on a solid surface,⁷ the numerical simulation was fairly consistent with experimental observation qualitatively. Hereby, in the present study, we would like to have a quantitative comparison between our thermodynamic model prediction and the experimental data. The configuration used in the present study is the capillary rise of a liquid in a small diameter tube. In order to illustrate our thermodynamics formulation without involving too much fluid mechanics content related to the singularity issue, we used a simplified fluid field inside the liquid. It is proved by using the second set of experimental data that this simplification leads to an acceptable deviation from the exact formulation (Sec. VI).

Let us outline our presentation in following sections before we go into the details. First of all, we apply the nonequilibrium thermodynamics framework to a gas/liquid/solid system which includes all the interfaces and triple-point-line. The fluid field is excluded from our system, yet it contributes to the solution of the problem via the Laplace pressure on the gas/liquid interface. Since there is no standard numerical scheme for the proposed nonequilibrium thermodynamics framework, in Sec. IV we present a Galerkin scheme for the numerical simulation under the thermodynamics framework. In Sec. V we interpret all the general formulations specifically to the capillary rise configuration. The fluid field is obtained under certain simplifications for this specific problem. The numerical results via the Galerkin scheme for the capillary rise problem, namely, the triple-point-line motion and gas/liquid interface change during the evolution, are pre-

sented in this section. In Sec. VI we present the experimental test setup and results of the capillary rise for two different geometric dimensions. The purpose of taking two geometric dimensions is to prove that the two material constants, mobility of gas/liquid interface and contact line, introduced in the thermodynamics formulation are truly the material dependent constants rather geometric dependent. The first test on the diameter of 0.73 mm tube is used to determine the two mobility constants, while the second test on the diameter 1.05 mm tube is then used as verification. In the last section, we make some comments on the present theory and existing models for the contact line and contact angle based upon our numerical and experimental results presented in the first few sections.

II. NONEQUILIBRIUM THERMODYNAMICS FORMULATION

The present modeling for contact line moving in a gas/liquid/solid system is based on the framework of nonequilibrium thermodynamics.^{8,9} Consider a gas/liquid/solid system, illustrated in Fig. 1(a). A liquid is in contact with a smooth and horizontal solid surface with gas/liquid, liquid/solid and gas/solid interfaces that conjoin at a contact line. Figure 1(c) shows a droplet spreading on a smooth solid surface as an example of the gas/liquid/solid system. The solid is assumed not to dissolve or otherwise react with the liquid. The interfaces change and the contact line motion are considered here in terms of thermodynamics formulation. Our thermodynamics system includes all the interfaces and the contact line only. The volume phases of the gas and liquid as well as solid are considered by their actions to the interfaces and contact line.

Nonequilibrium thermodynamics requires that the system changing is the process of the evolution of the system reducing its Gibbs free energy towards its minimum value. For the system under our consideration, the evolution of the interfaces S_{i-j} and the motion of contact line are driven by the change of the Gibbs free energy of the considered system, denoted by G hereafter. It comes from the sum of the interface energies among different phases, denoted by U , and the negative work supply W to the system by the external actions of the system. That is,

$$G = U - W, \quad (2.1)$$

with

$$U = \gamma_{1-2}A_{1-2} + \gamma_{1-3}A_{1-3} + \gamma_{2-3}A_{2-3}, \quad (2.2)$$

where γ_{i-j} is the specific surface tension and A_{i-j} is the area of the interface S_{i-j} between phase i and phase j , with phases 1, 2 and 3 denoting the liquid, the solid and the gas surrounding the liquid, respectively, as shown in Fig. 1(a) and Fig. 1(c) as an example.

A. Motion of gas/liquid interface and triple point line

The free energy by itself is not sufficient to determine the evolution of the gas/liquid/solid system, because countless ways of evolving processes would reduce the free energy. To describe the process of the contact line motion and

interfaces changes, more ingredients are needed.

Figure 1(b) illustrates the motion of the interface S_{1-3} between the liquid and the gas, and the motion of triple point line (TPL) at the junction of the liquid, the solid and the gas. A virtual motion of the interface S_{1-3} is a small movement in the direction normal to the interface that may not obey any kinetic law. The magnitude of the virtual motion, δr_n , can differ from point to point over the interface. Similarly, a virtual motion of the TPL is a small movement in the direction normal to the TPL in the solid surface that also need not obey any kinetic law. Again, the magnitude of the virtual motion of the TPL denoted by $\delta r_n^{(t)}$ can differ from point to point along the TPL.

Since the surface tension is assumed to be isotropic in the present study, the gas/liquid interface at a given time is usually a smooth surface. The area of a surface element is denoted by dA , the length of a line element by dl and the unit vector normal to the surface by \mathbf{n} , directing to the air phase. Of our particular interest is the sum of the two principal curvatures,

$$\kappa = \frac{1}{R_1} + \frac{1}{R_2}, \quad (2.3)$$

where R_1 and R_2 are the principal radii of curvature, taken to be positive for a convex surface. Associated with the virtual motion, δr_n , the area of the interface S_{1-3} varies by

$$\delta A_{1-3} = \iint_{S_{1-3}} \kappa \delta r_n dA. \quad (2.4)$$

These integrals extend over the interface S_{1-3} . Similarly, associated with the virtual motion of the TPL, $\delta r_n^{(t)}$, the area of the interface S_{1-3} varies by

$$\delta A_{1-3} = \oint_{L_t} \delta r_n^{(t)} \cos \theta dA, \quad (2.5)$$

and the areas of the interface S_{1-2} and S_{2-3} vary by

$$\delta A_{1-2} = \oint_{L_t} \delta r_n^{(t)} dl, \quad (2.6)$$

and $\delta A_{2-3} = -\delta A_{1-2}$, respectively. In Eq. (2.5) θ is the instant contact angle at any point on the TPL and the integral extends along the TPL, denoted by L_t .

During the evolution process of the TPL and the interfaces, it is noted that the virtual motions of S_{1-3} at any point on the TPL at any time must be satisfied with the following compatibility condition [Ref. Fig. 1(b)]:

$$\delta r_n = \delta r_n^{(t)} \sin \theta, \quad \text{on } L_t. \quad (2.7)$$

B. Driving forces and kinetic laws

Associated with the virtual motions, the free energy of the system varies by δG . Define the thermodynamic force on the liquid/gas interface, f , that drives the interface motion and the force on the TPL, f_t , that drives the TPL motion, as the free energy decreases with respect to the virtual motions,

$$\oint_{L_t} f_t \delta r_n^{(t)} dl + \iint_{S_{1-3}} f \delta r_n dA = -\delta G. \quad (2.8)$$

Since the virtual motion δr_n is an arbitrary function of the position on the interface S_{1-3} and the $\delta r_n^{(t)}$ is also an arbitrary function of the position on the line L_t , Eq. (2.8) uniquely defines the quantity f at every point on the interface S_{1-3} and the f_t at every point on the TPL L_t . The above-defined thermodynamic force f has a unit of stress (force/area) and f_t has a unit of surface tension (force/length), they are called driving forces of the dynamic system.

Let v_n and $v_n^{(t)}$ be the actual velocity of the interface S_{1-3} and the TPL L_t , respectively. Under the framework of a thermodynamic system, the actual velocities are taken to be functions of the driving forces. Specifically, the velocity is assumed to be linearly proportional to the driving force, i.e.,

$$v_n^{(t)} = M_t f_t, \quad (2.9a)$$

$$v_n = M f. \quad (2.9b)$$

Here M_t and M are called the mobilities of the TPL and the interface S_{1-3} , respectively. These two quantities are used as phenomenological parameters in the present analysis, to be determined by comparing theoretical predictions with experimental measurements. Since thermodynamics requires that the liquid surface move in the direction that reduces the free energy of the system, both of M_t and M are positive. Equations (2.9a) and (2.9b) are so-called the kinetic laws for the TPL and the interface.

It should be mentioned that the kinetic laws, (2.9a) and (2.9b) are linear and local relations. In other words, the velocity at a point only linearly depends on the forces at this point. The kinetic laws may be extended to nonlinear and nonlocal relations, where more constitutive parameters are needed to describe the system. In any case, the validity of the constitutive relations depends on the agreement between the theoretical prediction based on the assumed constitutive equations and the corresponding experimental observation. In the present analysis, we assumed the kinetic laws to be Eqs. (2.9a) and (2.9b) and both M_t and M are uniform and isotropic material parameters as the first attempt. Fortunately, the excellent agreement between our theoretical prediction and experimental results shows that Eqs. (2.9a) and (2.9b) is valid for the capillary flow in a thin tube. There should be no conceptual difficulties to extend the present framework to nonlinear and nonlocal theories.

The free energy, motion descriptions, driving forces and kinetic laws discussed above define the dynamics of the system evolution. In our later numerical scheme, the variation of the free energy of the system determines the driving forces at a given time; then the kinetic laws update the gas/liquid surface shape and the contact line position for a small time step. The process repeats for many time steps to evolve the interface shape to its equilibrium shape and the TPL to its equilibrium position.

III. MOTION EQUATIONS AND EQUILIBRIUM CONDITIONS

From Eqs. (2.1) and (2.2), the free energy change of the gas/liquid/solid system can be expressed by

$$\delta G = \gamma_{1-2} \delta A_{1-2} + \gamma_{1-3} \delta A_{1-3} + \gamma_{2-3} \delta A_{2-3} - \delta W. \quad (3.1)$$

Moreover, when the interface S_{1-3} moves by virtual motion δr_n and the TPL, L_t , moves by $\delta r_n^{(t)}$, the area changes δA_{i-j} of interfaces S_{i-j} are given by Eqs. (2.4)–(2.6). At the same time, the external work changes by $\delta W = \iint_{S_{1-3}} \Delta p \delta r_n dA$, where Δp is the pressure difference across the surface S_{1-3} , the so-called Laplace pressure. Consequently, associated with the virtual motions of the TPL and the interface, the free energy changes by

$$\begin{aligned} \delta G = & \oint_{L_t} \gamma_{1-2} \delta r_n^{(t)} dl - \oint_{L_t} \gamma_{2-3} \delta r_n^{(t)} dl \\ & + \oint_{L_t} \gamma_{1-3} \delta r_n^{(t)} \cos \theta dl + \iint_{S_{1-3}} \gamma_{1-3} \kappa \delta r_n dA \\ & - \iint_{S_{1-3}} \Delta p \delta r_n dA. \end{aligned} \quad (3.2)$$

A comparison of Eqs. (2.8) and (3.2) gives the expressions of the driving forces:

$$f_t = \gamma_{2-3} - \gamma_{1-2} - \gamma_{1-3} \cos \theta, \quad (3.3a)$$

$$f = \Delta p - \kappa \gamma_{1-3}. \quad (3.3b)$$

Equation (3.3a) expresses the driving force on the TPL in terms of the instant contact angle θ , and surface tension, γ_{i-j} . It has a clear physical meaning that f_t is the sum of the surface tensions projected along the unit vector normal to the TPL in the surface of the solid. Equation (3.3b) expresses the driving force on the interface in terms of the instant curvature κ , and the external action, Δp , as well as the surface tension, γ_{1-3} .

A combination of Eqs. (2.9) and (3.3) leads to

$$v_n^{(t)} = M_t (\gamma_{2-3} - \gamma_{1-2} - \gamma_{1-3} \cos \theta), \quad (3.4a)$$

$$v_n = M (\Delta p - \kappa \gamma_{1-3}). \quad (3.4b)$$

These partial differential equations govern the motions of the TPL and the liquid/gas interface during the system evolution process. The motion of contact line and the change of the interfaces depend on the solution of the set of motion equations (3.4) under the compatibility condition (2.7) and certain initial-value and boundary conditions.

At the end of the evolution process, the system reaches an equilibrium state. At that time, the free energy of the system achieves the minimum value, the liquid/gas interface shape and contact line position maintain unchanged, the contact angle arrives at its static value and the driving forces vanish. Setting $f_t = 0$ and $f = 0$ in Eq. (3.3) results in the equilibrium conditions for the TPL and the interface as

$$\gamma_{2-3} - \gamma_{1-2} - \gamma_{1-3} \cos \theta_e = 0, \quad (3.5a)$$

$$\Delta p - \kappa_e \gamma_{1-3} = 0, \quad (3.5b)$$

where θ_e and κ_e are the contact angle and the curvature in the equilibrium state, respectively. Equations (3.5a) and (3.5b) are the well-known Laplace–Young equations. They are frequently used to calculate the balance height of the meniscus above the flat liquid surface in the container in the capillary rise method to measure liquid–vapor interface energy (see e.g., Ref. 10).

IV. WEAK STATEMENT AND GENERALIZED COORDINATES

It is quite formidable to solve the set of the equation (3.4) in addition to certain specific conditions because of their nonlinear features. Therefore, a nonlinear dynamic system in the present case is formulated by a weak statement, which makes a standard numerical calculation possible.

Replacing the driving forces, f_i and f , in Eq. (2.8) with the velocities, $v_n^{(t)}$ and v_n , of the TPL and the interface by using the kinetic laws (2.9), gives

$$\oint_{L_t} \frac{v_n^{(t)}}{M_t} \delta r_n^{(t)} dl + \int \int_{S_{1-3}} \frac{v_n}{M} \delta r_n dA = -\delta G. \quad (4.1)$$

This is the so-called weak statement for a dynamic system. It means that the actual velocities, $v_n^{(t)}$ and v_n , must satisfy Eq. (4.1) for any of the arbitrary distributions of virtual motions, $\delta r_n^{(t)}$ and δr_n , on the TPL and the interface S_{1-3} , respectively. The weak statement is equivalent to the virtual work principle commonly studied in dynamics. Both of them lead to the Galerkin method in numerical implementation.

Let both of the liquid surface, S_{1-3} , and the TPL, L_t be described by m generalized coordinates, $\mathbf{q} = \{q_1, q_2, \dots, q_m\}$, and the corresponding generalized velocities, $\dot{\mathbf{q}} = \{\dot{q}_1, \dot{q}_2, \dots, \dot{q}_m\}$. Based on the differential geometry, the evolving surface S_{1-3} can be expressed by the position vector on the surface, $\mathbf{x} = \mathbf{x}(t)$, at a given time, then the position vector can be expressed as $\mathbf{x} = \mathbf{x}(q_1, q_2, \dots, q_m)$ by the generalized coordinates with the time implicitly contained in the generalized coordinates. Similarly, the position vector, $\mathbf{x}^{(t)}$, on the TPL in the surface of the inner tube wall can also express the moving TPL, namely, $\mathbf{x}^{(t)} = \mathbf{x}^{(t)} \times (q_1, q_2, \dots, q_m)$. Therefore, the virtual motions, $\delta r_n^{(t)}$ and δr_n , are linear in the variations of the generalized coordinates, i.e.,

$$\delta r_n^{(t)} = \sum_{i=1}^m \left(\mathbf{n}^{(t)} \cdot \frac{\partial \mathbf{x}^{(t)}}{\partial q_i} \right) \delta q_i \equiv \sum_{i=1}^m N_i^{(t)} \delta q_i, \quad (4.2a)$$

$$\delta r_n = \sum_{i=1}^m \left(\mathbf{n} \cdot \frac{\partial \mathbf{x}}{\partial q_i} \right) \delta q_i \equiv \sum_{i=1}^m N_i \delta q_i. \quad (4.2b)$$

Here, $N_i^{(t)}$ and N_i , the shape functions, depend on the generalized coordinates but not on the generalized velocities. Moreover, the actual velocities, $v_n^{(t)}$ and v_n , are linearly related to the generalized velocities, namely,

$$v_n^{(t)} = \sum_{i=1}^m N_i^{(t)} \dot{q}_i, \quad v_n = \sum_{i=1}^m N_i \dot{q}_i. \quad (4.3)$$

The generalized forces, f_1, f_2, \dots, f_m , conjugating to the generalized coordinates, are the differential coefficients of the free energy,

$$f_i = -\frac{\partial G}{\partial q_i}, \quad (4.4)$$

and the free energy variation is

$$\delta G = \sum_{i=1}^m \left(\frac{\partial G}{\partial q_i} \delta q_i \right) = -\sum_{i=1}^m f_i \delta q_i. \quad (4.5)$$

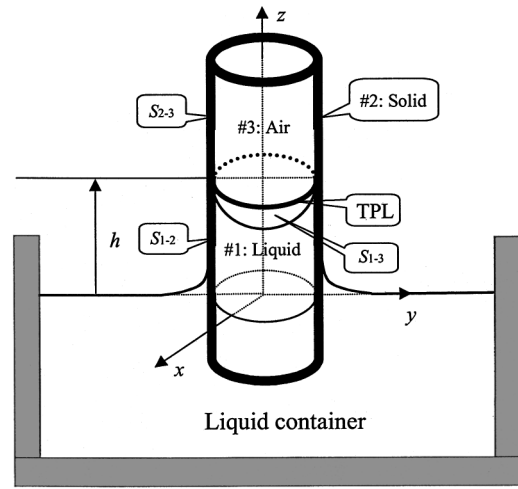


FIG. 2. The TPL and interfaces in the capillary rise process.

Here the generalized force, f_i , can be obtained by comparing the equation (4.5) with the result from substituting (4.2) into (3.2) as

$$f_i = \oint_{L_t} f_i N_i^{(t)} dl + \int \int_{S_{1-3}} f N_i dA. \quad (4.6)$$

Substituting the equations, (4.2), (4.3), and (4.5), into the weak statement (4.1) gives

$$\sum_{i,j=1}^m H_{ij} \dot{q}_j \delta q_i = \sum_{i=1}^m f_i \delta q_i, \quad (4.7a)$$

with

$$H_{ij} = \oint_{L_t} \frac{N_i^{(t)} N_j^{(t)}}{M_t} dl + \int \int_{S_{1-3}} \frac{N_i N_j}{M} dA. \quad (4.7b)$$

Bear in mind that the equation (4.7a) must be held for any virtual motion δq_i , so that

$$\sum_{j=1}^m H_{ij} \dot{q}_j = f_i, \quad i = 1, 2, \dots, m. \quad (4.8)$$

It can be seen from Eqs. (4.6) and (4.7b) that f_i and H_{ij} depend on the generalized coordinates $\{q_i\}$ nonlinearly. Therefore, the equations (4.8) is a set of nonlinear ODEs, which furnishes a dynamic system with the generalized coordinates $\{q_i\}$ to govern the process of the microscopic surface's evolution and the TPL motion driven by surface tensions and gravity.

V. IMPLEMENTATION OF THERMODYNAMICS FRAMEWORK TO CAPILLARY RISE FLOW

As an application of the proposed thermodynamics formulation for the gas/liquid/solid system, the movement of a meniscus in a capillary tube^{11,12} is especially considered in this section. As shown in Fig. 2, the capillary tube is of a circular cross-section and the inner diameter is very small, but the liquid container is sufficiently large so that the liquid volume change due to capillary rise is negligible. Meanwhile, it is assumed that the tube material readily wets the

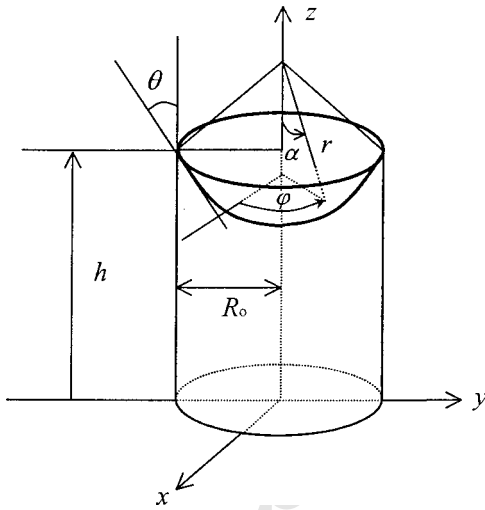


FIG. 3. The schematic diagram of the coordinate system.

liquid and does not dissolve or otherwise react with it. When a capillary tube is inserted into the liquid container vertically, the liquid/air interface in the tube first experiences a rapid rising and shape changing then followed by a very slow movement before it reaches the equilibrium position.

A. The system of generalized coordinates

The first problem to resolve this capillary flow is to describe the shape of the liquid/air interface. Generally speaking, describing an unknown surface shape needs many parameters. However, according to our experience,⁷ the numerical calculation time increases substantially as the number of parameters increase. Therefore, without losing the basic features of the problem, we describe the liquid/air interface with as few as possible parameters to simplify the formidable mathematical solution. Since the capillary flow is an axis-symmetry problem, we describe the shape of the surface S_{1-3} at a given time t by the following equations in the coordinate system illustrated in Fig. 3.

$$\begin{aligned} x &= r \sin \alpha \cos \varphi, \\ y &= r \sin \alpha \sin \varphi, \\ z &= h + r \sin \theta - r \cos \alpha. \end{aligned} \quad (5.1)$$

Here we assumed that the surface S_{1-3} is spherical in shape. Under this assumption, all the geometrical variables, such as the area of a surface element dA , the unit vector, \mathbf{n} , normal to the surface element, and the instant curvature of the surface element, κ , can be derived from (5.1) at an arbitrary time. Furthermore, we can also see from (5.1) that the height and shape of the surface are characterized by the geometrical quantities h , r and θ in the parametric Equation (5.1) where $\alpha \in [-\alpha_0, \alpha_0]$ with $\alpha_0 = \pi/2 - \theta$ and $\varphi \in [0, 2\pi]$. Needless to say, the h , r and θ evolve with the time during the capillary flow process. The position vector $\mathbf{x} = \{x, y, z\}$ depends on the time with the time implicitly contained in the quantities $h(t)$, $r(t)$ and $\theta(t)$. Here it is noted that the radius r and the instant angle θ must fulfill the relationship as follows:

$$R_0 = r \cos \theta \quad \text{or} \quad \dot{r} = \frac{R_0 \sin \theta}{\cos^2 \theta} \dot{\theta}, \quad (5.2)$$

where R_0 is the inner radius of the capillary tube. Therefore, there are only two independent geometrical quantities, h and θ , in this evolution system concerned. In the present study, $\{h, \theta\}$ are chosen as the generalized coordinates for the capillary flow system and the corresponding generalized velocities are $\{\dot{h}, \dot{\theta}\}$.

B. Governing equations

A simple geometrical analysis based upon Eq. (5.1) gives the normal velocity of the liquid surface as

$$v_n = -\dot{r} + (\dot{h} + \dot{r} \sin \theta + r \cos \theta \dot{\theta}) \cos \alpha, \quad (5.3)$$

Substituting Eq. (5.2) into (5.3) gives

$$v_n = N_h \dot{h} + N_\theta \dot{\theta}, \quad (5.4a)$$

with

$$N_h = \cos \alpha, \quad (5.4b)$$

and

$$N_\theta = -\frac{R_0 \sin \theta}{\cos^2 \theta} + \frac{R_0 \sin^2 \theta}{\cos^2 \theta} \cos \alpha + R_0 \cos \alpha. \quad (5.4c)$$

Simultaneously, the velocity of the TPL is obtained as

$$v_n^{(t)} = \dot{h}. \quad (5.5)$$

For the sake of convenience, all the equations will be written in dimensionless form. All the variables having length dimension are normalized by the tube inner radius R_0 , and all the variables having the same dimension as the surface tension are normalized by a selected surface tension γ_0 . We choose $\gamma_0 = \gamma_{1-3}$ in this paper. Consequently, the dimensionless generalized coordinates are denoted as

$$\{q_i\} = \{h/R_0, \theta\} \quad (i=1,2), \quad (5.6)$$

and the dimensionless generalized velocities are written as $\{\dot{q}_i\}$.

The normal velocity of the surface S_{1-3} , Eq. (5.4), is rewritten as

$$v_n = R_0 \left(\sum_{i=1}^2 \tilde{N}_i \dot{q}_i \right) \equiv \sum_{i=1}^2 N_i \dot{q}_i, \quad (5.7a)$$

with

$$\{\tilde{N}_i\} = \{N_h, N_\theta/R_0\} \quad (i=1,2). \quad (5.7b)$$

Similarly, the TPL velocity (5.5) is also rewritten as

$$v_n^{(t)} = R_0 \left(\sum_{i=1}^2 \tilde{N}_i^{(t)} \dot{q}_i \right) \equiv \sum_{i=1}^2 N_i^{(t)} \dot{q}_i, \quad (5.8a)$$

with

$$\{\tilde{N}_i^{(t)}\} = \{1, 0\} \quad (i=1,2). \quad (5.8b)$$

Substituting Eqs. (5.7) and (5.8) into (4.8), with the help of Eqs. (4.6), (4.7b) and (3.3), we finally obtain

$$\sum_{i=1}^2 H_{ij} \frac{dq_i}{d\tilde{t}} = f_j, \quad j=1,2, \quad (5.9)$$

with

$$H_{ij} = \tilde{N}_i^{(t)} \tilde{N}_j^{(t)} + 2\chi \int_0^{a_0} \tilde{N}_i \tilde{N}_j \left(\frac{\sin \alpha}{\cos^2 \theta} \right) d\alpha \quad (5.10a)$$

and

$$f_j = \left(\frac{\gamma_{2-3}}{\gamma_0} - \frac{\gamma_{1-2}}{\gamma_0} - \frac{\gamma_{1-3}}{\gamma_0} \cos \theta \right) \tilde{N}_j^{(t)} + 2 \int_0^{a_0} \left[\frac{R_0 \Delta p}{\gamma_0} - \tilde{\kappa} \frac{\gamma_{1-3}}{\gamma_0} \right] \tilde{N}_j \left(\frac{\sin \alpha}{\cos^2 \theta} \right) d\varphi. \quad (5.10b)$$

Here we introduced a pair of dimensionless parameter χ and a characteristic time t_0 , i.e.,

$$\chi = \frac{R_0 M_t}{M}, \quad t_0 = \frac{R_0}{M_1 \gamma_0}, \quad (5.11)$$

and \tilde{t} in the equation (5.9) and $\tilde{\kappa}$ in the equation (5.10b) denote the dimensionless t and κ , respectively, such as $\tilde{t} = t/t_0$.

Before we make the integration for Eq. (5.9), the pressure difference across the surface S_{1-3} must be estimated. In order to simplify the solution, we presume that the liquid is an incompressible fluid of known constant density and viscosity and is in a state of quasi-steady laminar flow, the pressure difference is expressed via fluid mechanics (see, e.g., Ref. 13) as

$$\begin{aligned} \Delta p &= -\rho g h(t) - \frac{8\mu}{R_0^2} h(t) \dot{h}(t) \\ &= -\rho g q_1(t) - 8\mu q_1(t) \dot{q}_1(t), \end{aligned} \quad (5.12)$$

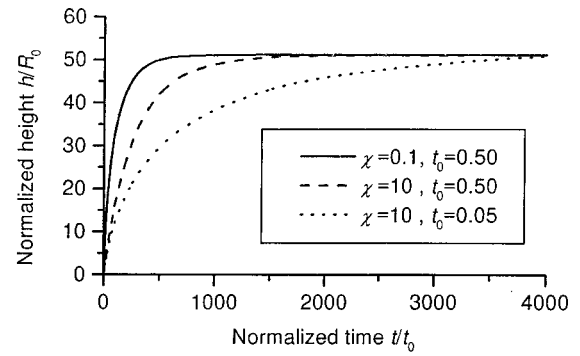
where ρg is the specific weight of the liquid and μ is the absolute viscosity. Here it should be noted that Eq. (5.12) is just a simplification of the solution under the assumption of quasi-steady laminar flow. For the capillary flow in a thin tube, this assumption is valid to a certain degree.¹⁴ The exact pressure field inside of the liquid can only be obtained by a more detailed fluid mechanics approach, which requires the solution for the issue of the shear stress singularity near the contact line as mentioned in the Introduction. This simplification is based on the fact that the motion of the fluid only plays a minor role in the energy change. Our later experimental observation proved this simplification

The instant curvature κ relate to the generalized coordinates via the following formula:

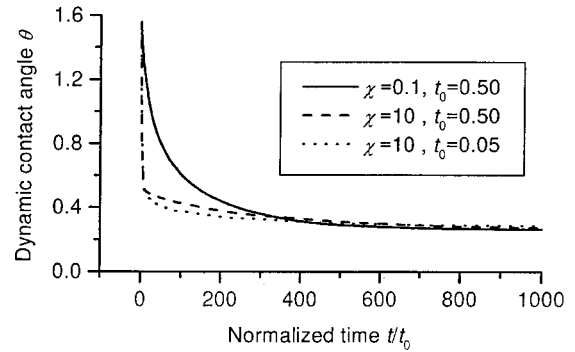
$$|\kappa| = |2 \cos \theta / R_0|. \quad (5.13)$$

From Eqs. (5.9) and (5.10), it is noted that the set of equations (5.9) furnishes a nonlinear dynamic system with the generalized coordinates $\{q_i\}$. The liquid surface rise and evolution during the capillary rise process depends on the solution of the set of (5.9) for given parameters: χ , t_0 , ρg and γ_{i-j} as well as the initial-value condition

$$q_i(\tilde{t})|_{\tilde{t}=0} = q_{i0} \quad (i=1,2), \quad (5.14)$$



(a) The dependence of the normalized height (h/R_0) on the normalized time (t/t_0)



(b) The dependence of the dynamic contact angle (θ) on the normalized time (t/t_0)

FIG. 4. Theoretical predictions for various parameters χ and t_0 .

where the initial values $\{q_{i0}\}$ describe the initial height and shape of the liquid surface. In other words, the set of the first order nonlinear equations (5.9) with the initial-value conditions (5.14) governs the capillary rise process.

C. Numerical results

Let us now consider the following case that the height and shape of the interface S_{1-3} at $t=0$ is

$$h(0) = 0, \quad \theta(0) = \theta_0. \quad (5.15)$$

Here θ_0 is the initial value of the instant contact angle $\theta(t)$. The Gear's method¹⁴ is adopted to solve the set of nonlinear ODEs (5.9) for $q_i(t)$. We have performed several case studies to check our numerical program and to illustrate the capillary rise phenomena.

The following numerical calculation is carried out for a comparison with the experimental results presented in the next section. All the geometrical dimensions and material constants are chosen to be consistent with our experimental setup. We consider the case of a normal engine oil in a glass tube of radius $R_0 = 0.365$ (mm) at atmospheric pressure. It has surface tension $\gamma_{1-3} = 0.0294$ (N m^{-1}), equilibrium contact angle $\theta_e = 15$ degrees and liquid weight density $\rho g = 8.33 \times 10^3$ (N m^{-3}) as well as absolute viscosity $\mu = 0.38$ ($\text{Pa} \cdot \text{s}$). The initial shape is given by (5.15) with $\theta_0 = \pi/2$. Figure 4 illustrates the numerical results for the above-mentioned oil with various parameters χ and t_0 . Fig-

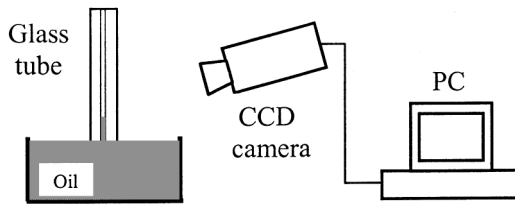


FIG. 5. Experimental setup for capillary flow measurement.

ure 4(a) shows the dependence of the normalized height h/R_0 on the normalized time t/t_0 , and Fig. 4(b) shows the dependence of the contact angle θ on the time t/t_0 , respectively.

From Fig. 4, it is clear that the meniscus shape change and TPL rising are extremely rapid at the beginning of the evolution, then followed by a slow rising process before it reaches the static equilibrium state. The comparison between dimensionless parameter $\chi=0.1$ and $\chi=10$ shows that the time duration to reach the static equilibrium state (denoted by t_e) for a small χ , is shorter than that for big χ . Actually, the normalized equilibrium times, t_e/t_0 , are estimated in the above numerical examples and they are 550 and 1500 for $\chi=0.1$, $t_0=0.5$ and $\chi=10$, $t_0=0.5$, respectively. As expected, the final static equilibrium heights are the same as for all two cases and it is the same as the computed equilibrium height of the liquid surface using the equilibrium conditions equation (3.5), namely, the well-known Laplace–Young equations.

VI. EXPERIMENTAL VERIFICATION

A. Experimental setup

An experiment was conducted to measure the dynamics of the capillary flow driven by the capillary force and balanced by the viscosity and the gravity forces. The experimental setup is shown in Fig. 5. It consists of a test tube, a liquid tank, a CCD camera and a PC for the picture capture and image processing. Two glass tubes were used in the experiment, whose inner diameters were, respectively, 0.73 (mm) and 1.05 (mm), measured by an optical inspection system. The glass tubes were cleaned by acetone before the testing to ensure good contact between the liquid and the inner surface of the tubes. Normal engine oil was used as the liquid and its viscosity was measured to be 0.38 (Pa·s). The other material constants are surface tension $\gamma_{1-3} = 0.0294$ (N m⁻¹), equilibrium contact angle $\theta_e = 15$ degrees and liquid weight density $\rho g = 8.33 \times 10^3$ (N m⁻³). The glass tubes were held vertically above the oil tank. The experiments were started by moving the tubes down to the oil surface in the tank and stayed still once the bottom of the tubes touched the oil. The capillary force would then drive the oil to move upwards along the tube until it was finally balanced by the gravity force. The whole processes were recorded by the CCD camera which was set at a frame grabbing speed of 6 frames/sec. The images were saved in the PC, from which the heights of the oil in the tubes at a different time were read.

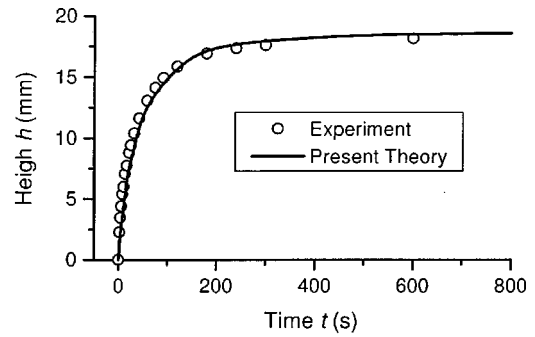
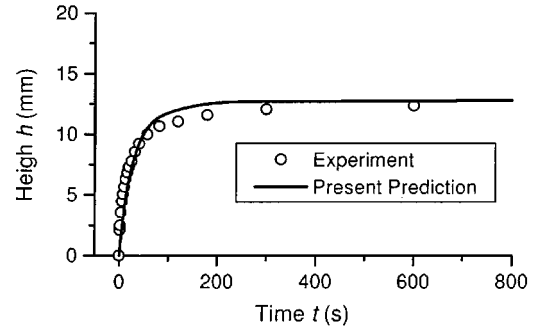
(a) $R_0=0.365$ mm(b) $R_0=0.525$ mm

FIG. 6. (a) The experimental data are used to calibrate M and M_t . (b) The analytical prediction agrees with the testing data.

B. Experimental results versus theoretical predictions

The material constants, the mobilities of the TPL and the surface (M_t and M) are normalized into a pair of dimensionless parameters χ and t_0 . The dependence of $h(t)$ curve on χ and t_0 is showed in Fig. 4(a). By fitting the experimental result for the case of $R_0=0.365$ (mm) shown in Fig. 6(a) with the theoretical results with various pairs (χ, t_0) , we obtain the pair with which the theory is in agreement with the experiment. Figure 6(a) illustrated the comparison between the experimental and theoretical result with $\chi=0.1$, $t_0=0.6$. Therefore, the materials constants, M_t and M , for the oil–glass system used in the experiment are given by Eq. (5.11) as

$$M_t = 2.07 \times 10^{-2} \text{ (m}^2 \text{N}^{-1} \text{S}^{-1}\text{)},$$

$$M = 7.55 \times 10^{-4} \text{ (m}^3 \text{N}^{-1} \text{s}^{-1}\text{)}.$$

With these measured mobilities, we made calculation for the case of $R_0=0.525$ (mm). The theoretical prediction is consistent with the experimental result in this case illustrated in Fig. 6(b).

VII. CONCLUDING REMARKS

In the present paper we proposed a nonequilibrium thermodynamics model for the gas/liquid/solid system. The time dependent process of the system evolution is described by the combination of contact line motion and the liquid/gas interface change driven by capillary forces. This process furnishes a nonlinear dynamic system and leads to a set of nonlinear ODEs with generalized coordinates. Two new material

constants, mobility M_t and M , are introduced in the formulation to describe the motion of contact line and evolution of the liquid/gas interface.

Both the analytical prediction given by the present thermodynamics model and experimental data showed that capillary flow process first experiences an extremely rapid rising and then followed by a slow rising before it reaches its static equilibrium position. A good agreement between our analytical prediction and experimental measurement [Fig. 6(b)] indicates that the nonequilibrium thermodynamics modeling is suitable for describing the gas/liquid/solid. Definitely, the thermodynamics model provides us a different angle from fluid mechanics methods to describe the gas/liquid/solid system. We believe it would be helpful in understanding the physical nature of the gas/liquid/solid system.

For more generalized thermodynamics system, we should include the energies from the flow of the liquid and gas. It becomes crucial for the problem in which the liquid flow is so complicated that there is no simplified solution that can be easily obtained. This will be left as future research work for us.

¹Y. D. Shikhmurzaev, "Moving contact line in liquid/liquid/solid systems," *J. Fluid Mech.* **334**, 211 (1997).

²P. Ehrhard and S. H. Davis, "Non-isothermal spreading of liquid drops on horizontal plates," *J. Fluid Mech.* **229**, 365 (1991).

³P. J. Haley and M. J. Miksis, "The effect of contact line on droplet spreading," *J. Fluid Mech.* **223**, 57 (1991).

⁴E. B. Dussan V, "The moving contact line: the slip boundary condition," *J. Fluid Mech.* **77**, 665 (1976).

⁵R. G. Cox, "Inertial and viscous effects on dynamic contact angles," *J. Fluid Mech.* **357**, 249 (1998).

⁶F. G. Yost, F. M. Hosking, and D. R. Frear, *The Mechanics of Solder Alloy Wetting and Spreading*, (Van Nostrand Reinhold, New York, 1993).

⁷Y. X. Gao, H. Fan, and Z. Xiao, "A thermodynamics model for solder profile evolution," *Acta Mater.* **48**, 863 (2000).

⁸S. R. de Groot and P. Mazur, *Non-Equilibrium Thermodynamics* (North-Holland, Amsterdam, 1962, Interscience, New York, 1962).

⁹Z. Suo, "Motion of microscopic surface in materials," *Adv. Mech.* **33**, 193 (1997).

¹⁰R. Trivedi and J. D. Hunt, "Surface and interface energy measurements," in *Proceedings of the Mechanics of Solder Alloy Wetting & Spreading*, edited by F. G. Yost, F. M. Hosking, and D. R. Frear (Van Nostrand Reinhold, New York, 1993), pp. 191–226.

¹¹E. W. Washburn, "The dynamics of capillary flow," *Phys. Rev.* **17**, 273 (1921).

¹²J. Lowndes, "The numerical simulation of the steady movement of a fluid meniscus in a capillary tube," *J. Fluid Mech.* **101**, 631 (1980).

¹³J. J. Bertin, *Engineering Fluid Mechanics*, 2nd ed. (Prentice–Hall, Englewood Cliffs, 1986).

¹⁴C. W. Gear, *Numerical Initial Value Problems in Ordinary Differential Equations* (Prentice–Hall, Englewood Cliffs, 1971).